ANALYSIS AND SIMULATION OF THE MELTING BEHAVIOR OF POLYMER MATERIALS IN CO-KNEADERS

Rudloff Johannes, Wilhelm Matthias, Lang Marieluise, Heidemeyer Peter, Bastian Martin

SKZ - German Plastics Center - Wuerzburg - Germany

ABSTRACT

The co-kneader is well known for its superior mixing performance and its exact temperature control capabilities. Therefore it is widely used in the polymer industry for the compounding of shear and temperature sensitive materials like PVC or high filled compounds. In contrast to the considerable amount of scientific work that deals with investigation, modeling or simulation of the process behavior of single and twin screw extruders there are only few publications about the co-kneader. Due to increased quality requirements and the trend for cost reduction by process optimization, this is increasingly becoming a problem for plant construction and processing companies.

To address this problem, experimental investigations of the melting behavior of polymer materials in the co-kneader had been conducted. In order to determine the melting degree along the extruder length a special barrel was used which can be opened in axial direction. Based on the experimental results, a theoretical consideration for co-kneaders that are operated as plastification extruders is proposed. At first the relevant process is divided into three parts consisting of solid conveying, melting initiation and melting propagation. The solid conveying is described by the Archimedes solid conveying model. In order to estimate the melting initiation the solid particles temperature increase is used for partially filled sections. Furthermore, it is assumed that the melting cannot start later than at the point where the extruder flow channels are fully filled for the first time. The melting propagation is described by a modified disperse melting model. The developed models are implemented into a simulation tool. A comparison between simulated results and experimental data shows a descent agreement.

Index Terms – Extrusion, compounding, planetary roller extruder, modelling

1. INTRODUCTION

The co-kneader is a compounding extruder that is based on a patent of Heinz List [1]. The extruder consists of a reciprocating single screw with interrupted flights that oscillates in a barrel containing pins in such a manner as to cause the pins to wipe the flights [2]. The modern kneader is modular in construction containing a range of different screw element arranged on a shaft. Beyond publications dealing with applications [2-6] there was little study of the basic process behavior of co-kneaders until the 1990s. In the 1990s Elemans and Meijer [7] as well as Lyu and White [8-11] dealt with the fluid mechanics, heat transfer and melting in co-kneaders. Elemans and Meijer developed a melt transporting model for Newtonian fluids including the axial movement and the pin influence. Lyu and White modeled the melt transporting for viscous non-Newtonian polymer melts [8-10] but neglected the pin influence.

Furthermore they performed experimental investigation of the residence time and melting [11]. There are several problems using the models for current development processes:

- The investigations were all performed on co-kneaders with 3-flighted mixing elements. Since 2007 there are also co-kneaders with 4-flighted mixing elements available. For these machines investigations are performed with the aim of process modelling.
- No models of the melting process in co-kneaders are known.
- The published models are not implemented in scientific or commercial simulation software.

To address these problems experimental investigations of a co-kneader with 4-flighted mixing elements are presented in this paper. Furthermore an approach for a comprehensive process modelling of the co-kneader is described and a melting model as part of this comprehensive model is presented.

2. EXPERIMENTAL INVESTIGATIONS

In order to investigate the process behavior of co-kneaders dead-stop-trials were performed. A Buss co-kneader type MX-30 was used. The extruder screw did consist of a solid conveying zone, a melting zone and two mixing zones, each separated by a melt conveying zone. As material a high density polyethylene type Sabic Vestolen 6060 N and a polystyrene type INEOS Styrolution 486 N were used. In the experiments shown here a throughput of 10 kg/h, a rotation speed of 400 1/min and a barrel temperature of 200 °C were selected. In order to separate solid particles and melt the pellets were dyed blue and yellow with a pigment in a previous compounding step. Therefore 0.75 % yellow pigment and 0.1 % blue pigment were used.

The results of the dead-stop-trials are shown in Figure 1. The extrusion direction is from left to right. Even if PS sticks more to the barrel than PE the process behavior for both materials is similar. There are solid conveying zones and fully and partially filled sections for both materials. The melting starts for both materials approximately at the first fully filled section. In this melting section no compact solid bed is found and a disperse melting mechanism occurred. PE is melting slower than PS because of its higher melting enthalpy. If a closer look is taken at the melt conveying, there are at first partially filled conveying elements upstream of the mixing sections. Then a short fully filled conveying element section of approximately 10 mm followed by a fully filled mixing element section occurs. Further downstream a partially filled conveying elements section follows. This indicates that the melt transport capacity of the conveying elements is high enough to transport the throughput given by the dosing unit. In contrast, the melt transport capacity of the mixing elements is not high enough to transport the throughput.
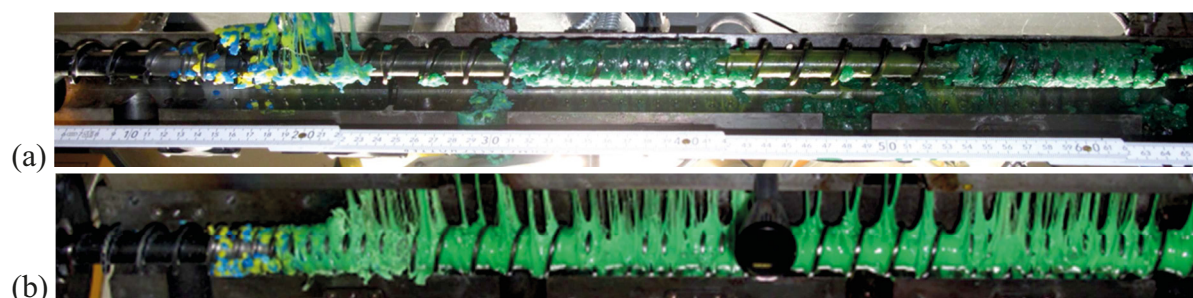

FIGURE 1. Results of the dead-stop-trials for PE (a) and PS (b)

3. MODELLING

In the first step the co-kneader is divided in small sections with constant geometry and temperature conditions along the extruder length. The length of these sections must be 1 mm or smaller. This allows a separate modelling for all processes like melt transport, temperature development or melting and coupling the single calculation steps in a Excel based simulation tool called "SimKo". Furthermore for coupling the separate process models, an iterative simulation process is performed in the simulation tool. This is a common process in the extrusion modelling that is also used for the simulation of single screw, co-rotating twin screw and planetary roller extruders [12-15].

3.1 Geometry model

The co-kneader is basically a single screw extruder, so the base geometry parameters of this extruder type as published by White and Potente [14] can be used. When looking at unrolled elements as shown in figure 2 we receive for example the geometry parameters channel width b and number of channels i_K.

(a)

(b)
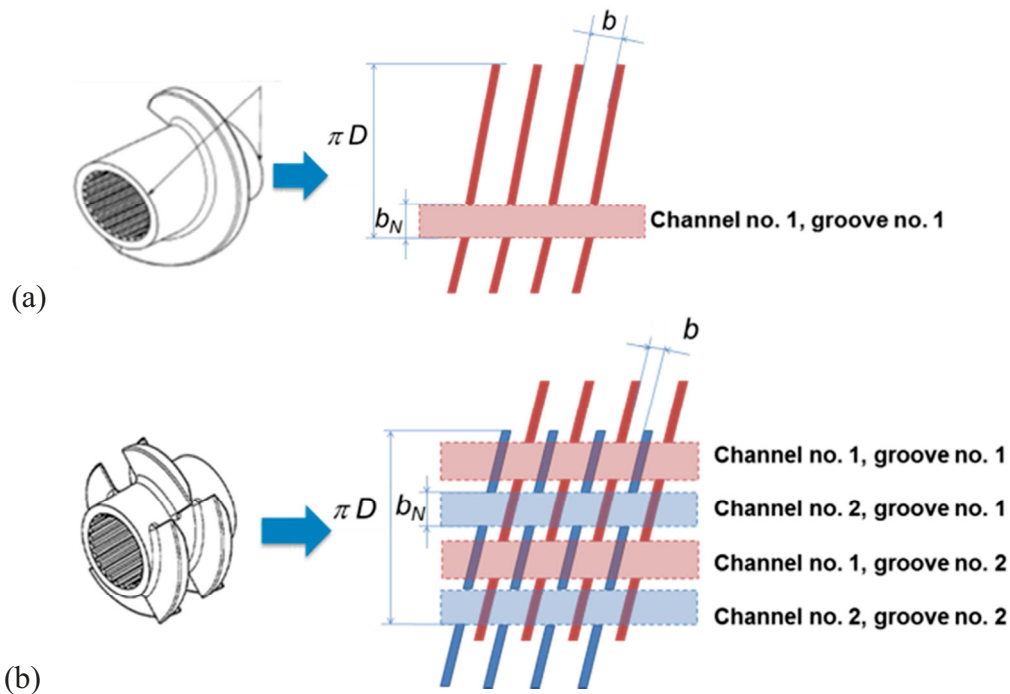
FIGURE 2. Schematically view of the groove geometry model of co-kneaders for conveying (a) and mixing (b) elements

The conveying element shown in figure 2 (a) consists of one channel, the mixing element in figure 2 (b) consist of two channels each with a width of b. These geometry parameters have to be extended by further geometry parameters to describe the grooves and pins of the kneader. Because one wants to neglect the pin influence in the first model, only the grooves in the first step needs to be described. Therefore groove width b_N and groove number i_N are used. The convening element has one groove in its one channel and the mixing element has two grooves in each of its two channels all with a width of b_N.

3.2 Melt conveying

In order to model the melt transport in co-kneaders the melt transport in channels and grooves are modelled separately and coupled by a pressure and volume flow balance. The influence of

pins and axial stroke are neglected in the first modeling step presented in this paper. It is assumed that the volume flow given by the dosing unit is the sum of the volume flow in each channel minus the volume flow in each groove:

$$\dot{V} = i_K \cdot \dot{V}_K - i_n \cdot \dot{V}_n \tag{1}$$

Furthermore it is assumed that the pressure difference is the same at each position along the channel direction (z-axis):

$$\frac{\Delta p}{\Delta z} = \frac{\Delta p_K}{\Delta z_K} = \frac{\Delta p_N}{\Delta z_N} \tag{2}$$

Then it is assumed that the melt transport can be described as a superposition of drag and pressure induced flow by dimensionless flow numbers established for rectangular channels. Therefore the equations shown in table 1 are used to describe the flow in channels and grooves

TABLE 1. Dimensionless operating numbers

	Extruder	**Channel**	**Groove**
Dimensionless volume flow	$\pi_{\dot{V}} = \dfrac{\dot{V}}{i_K \cdot 0{,}5 \cdot h \cdot b \cdot v \cdot \cos\beta}$	$\pi_{\dot{V},K} = \dfrac{\dot{V}_K}{0{,}5 \cdot h \cdot b \cdot v \cdot \cos\beta}$	$\pi_{\dot{V},N} = \dfrac{\dot{V}_N}{0{,}5 \cdot h_N \cdot b_N \cdot v \cdot \sin\beta}$
Dimensionless pressure gradient	$\pi_p = \dfrac{\Delta p}{\Delta z} \cdot \dfrac{h^{n+1}}{6 \cdot K \cdot (v \cdot \cos\beta)^n}$	$\pi_{p,K} = \dfrac{\Delta p}{\Delta z} \cdot \dfrac{h^{n+1}}{6 \cdot K \cdot (v \cdot \cos\beta)^n}$	$\pi_{p,N} = \dfrac{\Delta p}{\Delta z \cdot \tan\beta} \cdot \dfrac{h_N^{n+1}}{6 \cdot K \cdot (v \cdot \sin\beta)^n}$
Linking	Equation 3	$\pi_{\dot{V},K} = A_K - B_K \cdot \pi_{p,K}$	$\pi_{\dot{V},N} = A_N - B_N \cdot \pi_{Vp,N}$

The model parameters A_K, A_N, B_K and B_N can describe further influences on the flow like structure viscosity or screw pitch. By coupling the equations in table 1 with equation 1 and 2 we get equation 3 that describes the dimensionless volume flow of the co-kneader:

$$\pi_{\dot{V}} = A_K - A_N \cdot \tan\beta \cdot \frac{h_N \cdot b_N \cdot i_n}{h \cdot b \cdot i_k} - \left(B_K + B_N \cdot \frac{h_N^{n+2} \cdot b_N \cdot i_n}{\tan\beta^n \cdot h^{n+2} \cdot b \cdot i_k} \right) \cdot \pi_{p,K} \tag{3}$$

The velocity is calculated by equation 4 and the shear rate to calculate the viscosity parameters from the power law can be estimated by equation 5:

$$v = \pi \cdot D \cdot N_0 \tag{4}$$

$$\dot{\gamma} = \frac{h}{v \cdot \sin\beta} \tag{5}$$

If one sets all model parameters (A_K, A_N, B_K and B_N) on 1, which means that further influences like structure viscosity and cross flow are neglected, one gets pressure-throughput characteristics as shown in figure 3.
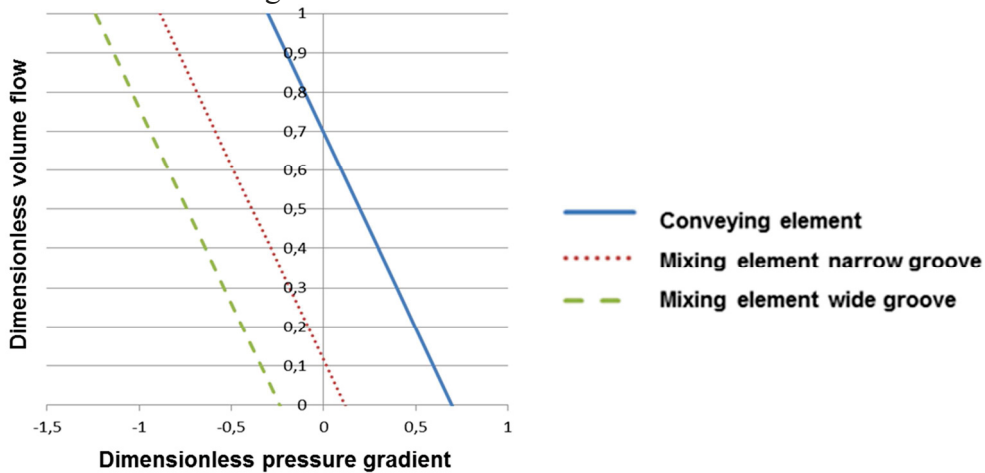
FIGURE 3. Pressure-throughput characteristics of co-kneader elements

A single screw extruder without grooves would be represented by a line from 1 on the y-axis to 1 on the x-axis. Because of the grooves the maximal volume flow and pressure gradient are decreasing. This is the reason why mixing elements in co-kneaders are fully filled in most of the operating points. The fully filled conveying element section upstream of the mixing elements builds up the pressure that is necessary to overcome the mixing elements.

For partially filled sections the filling degree f can be calculated with equation 6:

$$f = \frac{\pi_{\dot{V}}}{A_K - A_N \cdot \tan\beta \cdot \dfrac{h_N \cdot b_N \cdot i_n}{h \cdot b \cdot i_k}} \tag{6}$$

The average residence time in a section is given by equation 7:

$$\bar{t} = \frac{V \cdot f}{\dot{V}} \tag{7}$$

3.3 Solid conveying

As discussed in the geometry model section 3.1 the co-kneader geometry is similar to a single screw extruder, one difference to single screw extruders being that co-kneaders are usually operated in underfed conditions. Because of the similarity to a solids conveying section of the single screw extruder concept, the Archimedes solid conveying Model [14, 16] can be used.

$$\dot{m} = \rho_B \cdot A \cdot v_a \cdot f \tag{8}$$

In Equation 8 the throughput is given by the dosing unit and the filling degree has to be calculated. The cross section area is given by the geometry of the co-kneader in the feeding section and the bulk density is a material parameter that can be measured easily. The axial solids velocity is given by the rotation speed and the flight pitch for partially filled solid conveying sections of single screw extruders as shown in Equation 9:

$$v_a = t \cdot N_0 \tag{9}$$

3.4 Melting initiation

The experimental investigations showed that the melting starts at the latest when the solid particles reach the first fully filled section. Depending on the process conditions, the melting can start in the partially filled section as well. In order to estimate this case, the solid temperature development can be taken in account. Therefore a model that was developed by Jung for twin screw extruders [17] and was transferred to the planetary roller extruder in our previous work [15] is used for the kneader. In this model thermal conduction into material that has contact with the barrel surface is considered and melting can start when the temperature of material in contact with the barrel reaches the softening temperature. The temperature development of the material with barrel contact is described by equation 10:

$$\overline{T}_S(l) = a_B \cdot (T_B - T_0) \cdot \left(1 - e^{-\frac{2 \cdot a_B \cdot l}{\rho_S \cdot c_{p,S} \cdot v_a \cdot r_0}}\right) + T_0 \tag{10}$$

The melting starts, when the pellet temperature reaches the glass transition temperature for amorphous materials or the melting temperature for semi crystalline materials. If the screw is heated and the screw temperature is above the barrel temperature, the same procedure can be used, but the barrel temperature has to be replaced with the screw temperature.

3.5 Melting propagation

For melting propagation a disperse melting model is used. This model suits to the investigated operating point and is used for twin screw extruders [13] and planetary roller extruders [15] as well. In the disperse melting model, isolated solid particles in surrounding melt are observed. The solid particles are considered as spheres and ongoing melting leads to a reduction of the

radius of the spheres. The sphere radius then correlates with the melting degree and is described by equation 11:

$$r_{i+1} = \left\{ r_i^2 - \frac{2 \cdot \lambda_M}{\rho_S \cdot c_{p,M}} \cdot \ln\left(1 + \frac{c_{p,M} \cdot (T_M - T_{Fl})}{\Delta h}\right) \cdot \Delta \bar{t} \right\}^{\frac{1}{2}}$$

(11)

4. CONCLUSIONS

Simulated pressure, filling degree and melting degree profiles for PE (a) and PS (b) are shown in figure 4.
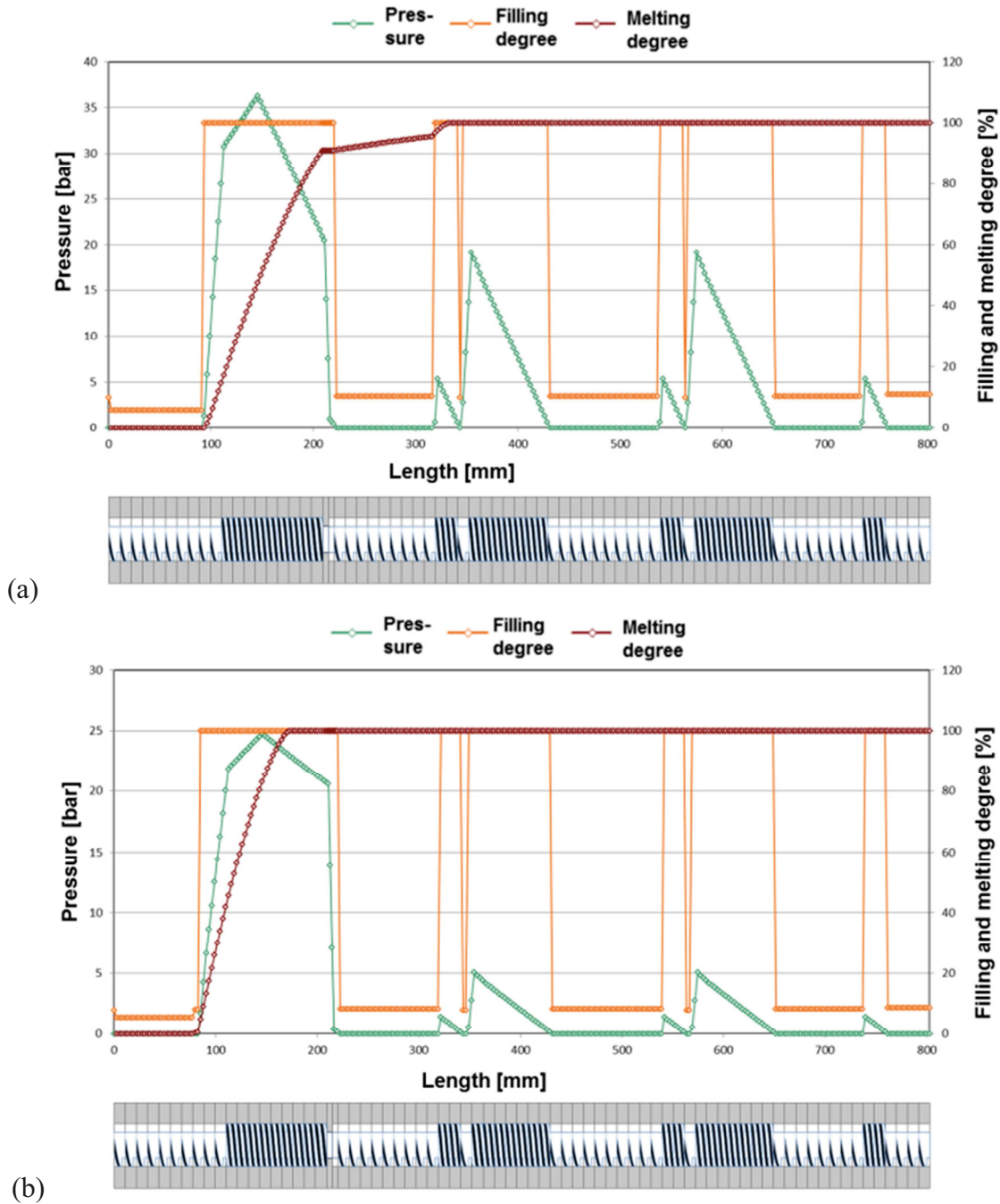

(a)

(b)

FIGURE 4. Simulated pressure, filling and melting degree profiles for PE (a) and PS (b)

In these simulations the melt temperature was set on the value of the barrel temperature. This was necessary because until now no temperature models have been developed for the co-kneader. The different melting length for PE and PS can be covered well. The simulated filling degrees show a good agreement with the experimental results, especially under consideration of the assumptions that were necessary for modelling. In the next step the models will be extended, so that they can cover pin, axial stroke, cross flow and structure viscosity influences. Therefore further experimental investigations are necessary. In this experiments pressure gradients and melting degrees along the melting and mixing sections will be measured for a wider range of operating conditions.

5. SYMBOLS

A	Cross section area	A_K	Model parameter	A_N	Model parameter
a_B	Heat transfer coefficient at the barrel	A_N	Model parameter	B_K	Model parameter
b	Channel width	b_N	Groove width	$c_{p,M}$	Spec. melt heat capacity
$c_{p,S}$	Spec. solid heat capacity	D	Screw Diameter	f	Filling degree
h	Channel height	h_N	Groove height	Δh	Melting enthalpy
i_K	Channel number	i_N	Groove number	K	Power law consistency factor
l	Axial length	$\dot{m}$	Throughput	r_0	Starting particle radius
r_i	Particle radius	N_0	Rotation speed	n	Power law flow exponent
Δp	Pressure gradient	T_0	Starting solid particle temperature	T_B	Barrel Temperature
T_{Fl}	Softening temperature	T_M	Melt temperature	$\overline{T}_S$	Average solid particle temperature
t	Flight pitch	$\bar{t}$	Residence time	$\Delta\bar{t}$	Residence time in a section
$\dot{V}$	Volume flow	$\dot{V}_K$	Channel volume flow	$\dot{V}_N$	Groove volume flow
v	Velocity	v_a	Axial solid velocity	Δz	Length gradient in channel direction
β	Channel pitch angle	λ_M	Thermal conductivity of the melt	ρ_B	Bulk density
ρ_S	Solid density	π_p	Dimensionless pressure gradient of the extruder	$\pi_{p,K}$	Dimensionless pressure gradient of the channel
$\pi_{p,N}$	Dimensionless volume flow of the groove	$\pi_{\dot{V}}$	Dimensionless volume flow of the extruder	$\pi_{\dot{V},K}$	Dimensionless volume flow of the channel
$\pi_{\dot{V},N}$	Dimensionless volume flow of the groove	$\dot{\gamma}$	Shear rate	$\pi_{\dot{V},N}$	Dimensionless volume flow of the groove

6. ACKNOWLEDGMENTS

REFERENCES

[1]   H. List, Swiss Patent No. 1945 247,704 (20 Aug 1947).
[2]   K. H. Stade, Polym. Eng. Sci. 17, 50–57 (1977).

[3] E. Schneider and D. H. M. Brooks, British Plastics, 30, 480 (1957).

[4] T. Timm, D. Stoltzenberg and H. Fettback, Kautschuk Gummi Kunst. 18, 206 (1965).

[5] D. B. Todd and J. W. Hunt, SPE ANTEC Tech Papers 19, 577 (1973).

[6] P. Schnottale, Kautschuk Gummi Kunst. 38 116 (1985).

[7] P. H. M. Elemans and H. E. M. Meijer, Polym. Eng. Sci. 30, 893-904 (1990).

[8] M. Y. Lyu and J. L. White, Int. Polym. Process. 10, 305– 313 (1995).

[9] M. Y. Lyu and J. L. White, Int. Polym. Process. 11, 208–221 (1996).

[10] M. Y. Lyu and J. L. White, Polym. Eng. Sci. 37, 623-635 (1997).

[11] M. Y. Lyu and J. L. White, Polym. Eng. Sci. 38, 1366–1377 (1998).

[12] B. Vergnes, G. Della Valle and M. Delamare, Polym. Eng. & Sci. 38, 1781–1792 (1998).

[13] A. Thümen, "Disperses Aufschmelzen in Doppelschneckenextrudern", Ph.D. thesis, University of Paderborn, 2008

[14] J. L. White and H. Potente, Screw Extrusion (Carl Hanser Verlag, Munich, 2002).

[15] J. Rudloff, M. Lang, K. Kretschmer, P. Heidemeyer, M. Bastian, M. Koch "A mathematical model describing the solid conveying and melting behavior of planetary roller extruders", AIP Conference Proceedings 1593, (American Institute of Physics, Melville, NY, 2014), pp. 592 – 595.

[16] K. Wilczyński; A. Lewandowski; K. J. Wilczyński, Polym. Eng. and Sci. 52, 1258–1270 (2012).

[17] J.L. White; H. Jung Inter. Polymer Processing 23, 242-251 (2008).

CONTACTS

J. Rudloff   j.rudloff@skz.de
M. Wilhelm   m.wilhelm@skz.de
M. Lang   m.lang@skz.de
P. Heidemeyer   p.heidemeyer@skz.de
M. Bastian   m.bastian@skz.de